

*Advances in particle acceleration at  
non-relativistic shocks: from plasma instabilities  
to entire supernova remnants*

Christoph Pfrommer<sup>1</sup>

in collaboration with

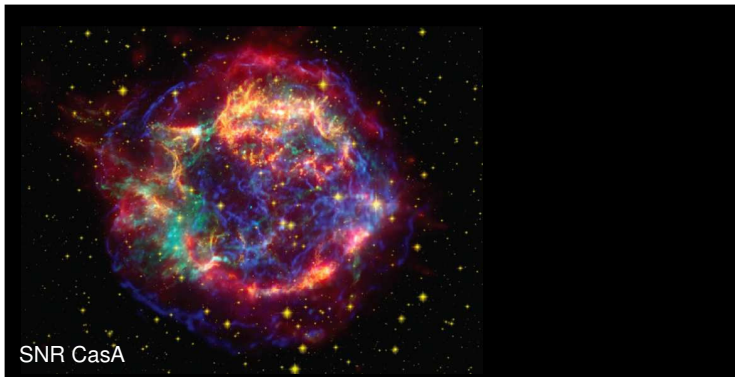
PhD students: K. Ehlert,<sup>1</sup> L. Jlassi,<sup>1</sup> **R. Lemmerz**,<sup>1</sup> **T. Thomas**,<sup>1</sup>  
M. Werhahn,<sup>1</sup> J. Whittingham,<sup>1</sup> **G. Winner**<sup>1</sup>  
T. Berlok,<sup>1</sup> P. Girichidis,<sup>2</sup> **M. Pais**,<sup>3</sup> R. Pakmor,<sup>4</sup> **M. Shalaby**,<sup>1</sup> M. Sparre<sup>5,1</sup>

<sup>1</sup>AIP Potsdam, <sup>2</sup>U of Heidelberg, <sup>3</sup>Hebrew U, <sup>4</sup>MPA Garching, <sup>5</sup>U of Potsdam

PASTO2022, Rome, Sep 2022



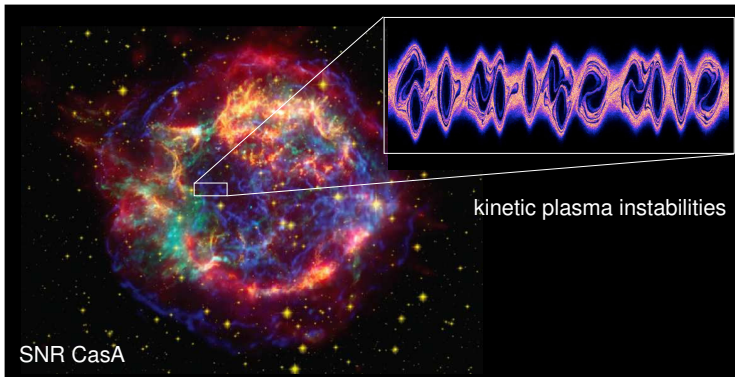
# Particle acceleration: an extreme multi-scale problem



supernova remnant:

$$r_{\text{SNR}} \sim 3 \text{ pc} \sim 1 \times 10^{19} \text{ cm},$$

# Particle acceleration: an extreme multi-scale problem



supernova remnant:

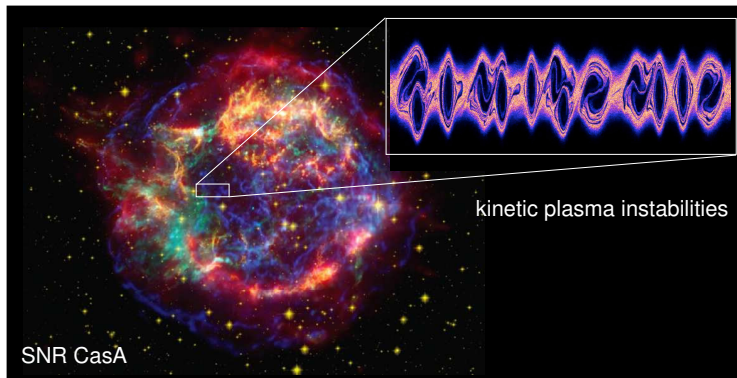
$$r_{\text{SNR}} \sim 3 \text{ pc} \sim 1 \times 10^{19} \text{ cm},$$

plasma skin depth:

$$\lambda_i = \frac{c}{\omega_i} \sim 2 \times 10^7 \left( \frac{n}{1 \text{ cm}^{-3}} \right)^{-1/2} \text{ cm}$$



# Particle acceleration: an extreme multi-scale problem



supernova remnant:

$$r_{\text{SNR}} \sim 3 \text{ pc} \sim 1 \times 10^{19} \text{ cm},$$

plasma skin depth:

$$\lambda_i = \frac{c}{\omega_i} \sim 2 \times 10^7 \left( \frac{n}{1 \text{ cm}^{-3}} \right)^{-1/2} \text{ cm}$$

⇒ need to develop a **multi-scale approach: PIC and MHD models!**

# Outline

- 1 Cosmic ray driven instabilities
  - Introduction
  - Intermediate instability
  - Overview and applications
- 2 Electron acceleration at shocks
  - The problem
  - Electron acceleration
  - Intermediate-scale instability at shocks
- 3 Supernova remnant simulations
  - MHD setup
  - Protons and hadronic emission
  - Electrons and leptonic emission



# Cosmic ray scattering with background plasma

- **extrinsic confinement:** scattering off of turbulence injected on the driving scale and cascaded to smaller scales  
⇒ **important for confinement of TeV CRs**



# Cosmic ray scattering with background plasma

- **extrinsic confinement:** scattering off of turbulence injected on the driving scale and cascaded to smaller scales  
⇒ **important for confinement of TeV CRs**
- **intrinsic confinement:** CRs drive unstable plasma wave modes (e.g., Alfvén waves), and then scatter off of them  
⇒ **most important mechanism for GeV CR confinement**



# Cosmic ray scattering with background plasma

- **extrinsic confinement**: scattering off of turbulence injected on the driving scale and cascaded to smaller scales  
 ⇒ **important for confinement of TeV CRs**
- **intrinsic confinement**: CRs drive unstable plasma wave modes (e.g., Alfvén waves), and then scatter off of them  
 ⇒ **most important mechanism for GeV CR confinement**
- **dispersion relation** ( $\Omega_{e,0} = -m_i/m_e \times \Omega_{i,0}$ ,  $\alpha = n_{cr}/n_i$ ): gyrotropic CR ion + electron beam propagates in background plasma

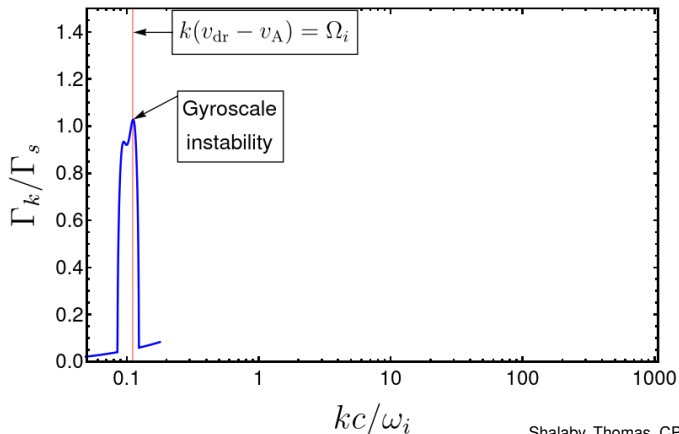
$$\frac{k^2 c^2}{\omega^2} - 1 = \frac{\omega_i^2}{\omega(-\omega \pm \Omega_{i,0})} + \frac{\omega_e^2}{\omega(-\omega \pm \Omega_{e,0})} \quad \leftarrow \text{background}$$

$$\text{CRe} \Rightarrow + \frac{\alpha \omega_e^2}{\gamma_e \omega^2} \left\{ \frac{\omega - kv_{dr}}{kv_{dr} - \omega \mp \Omega_{e,0}/\gamma_e} \right\}$$

$$\text{CRi} \Rightarrow + \frac{\alpha \omega_i^2}{\gamma_i \omega^2} \left\{ \frac{\omega - kv_{dr}}{kv_{dr} - \omega \pm \Omega_i} - \frac{v_{\perp}^2 (k^2 c^2 - \omega^2) / c^2}{2 (kv_{dr} - \omega \pm \Omega_i)^2} \right\}$$



# CR driven instabilities – growth rates

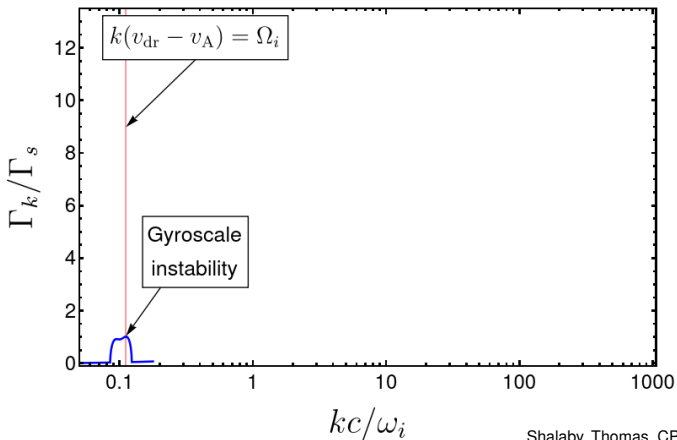


Shalaby, Thomas, CP (2021)

- gyro-resonant instability of gyrotropic CR population



# CR driven instabilities – growth rates

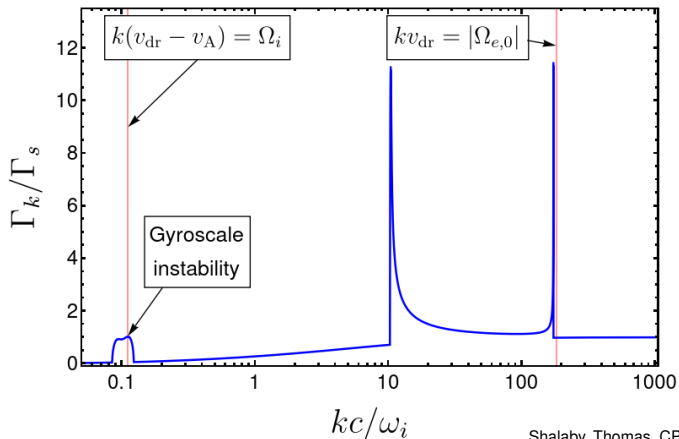


Shalaby, Thomas, CP (2021)

- gyro-resonant instability of gyrotropic CR population



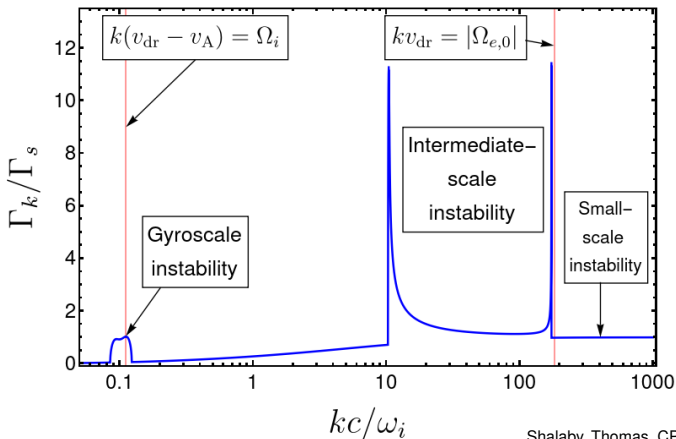
# CR driven instabilities – growth rates



Shalaby, Thomas, CP (2021)

- **new intermediate-scale instability** of gyrotropic CR population

# CR driven instabilities – growth rates

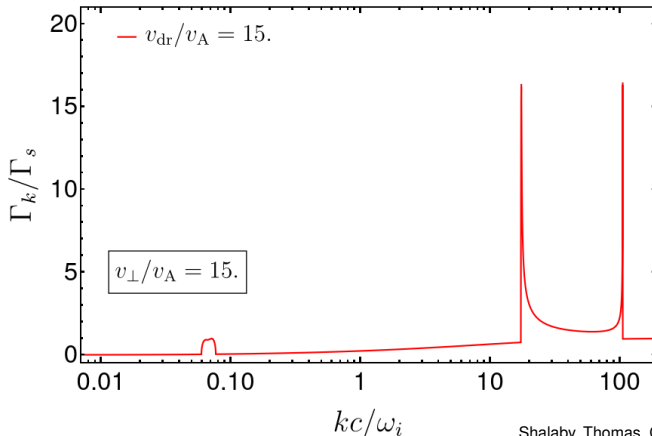


Shalaby, Thomas, CP (2021)

- **new intermediate-scale instability** of gyrotropic CR population



# CR driven intermediate-scale instability

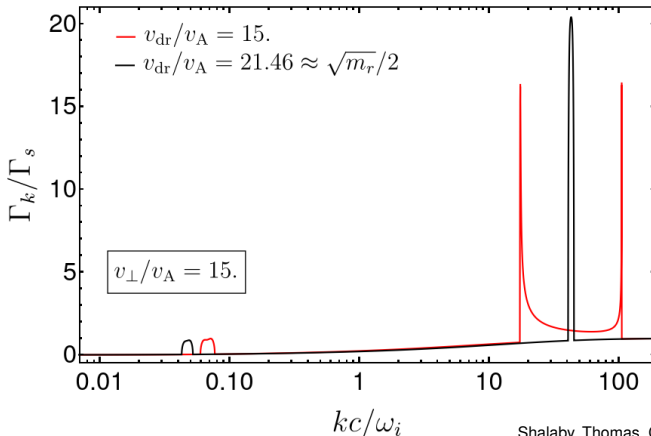


Shalaby, Thomas, CP (2021)

- low CR drift speed: two instability peaks



# CR driven intermediate-scale instability

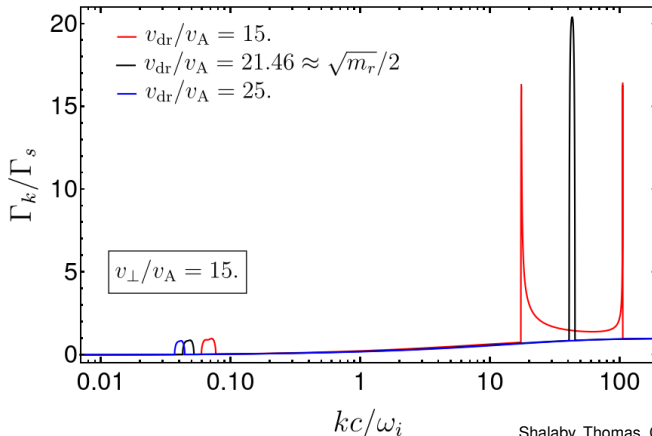


Shalaby, Thomas, CP (2021)

- for CR drift speed  $v_{dr} \approx \sqrt{\frac{m_i}{m_e}} \frac{v_A}{2}$ : two instability peaks merge



# CR driven intermediate-scale instability



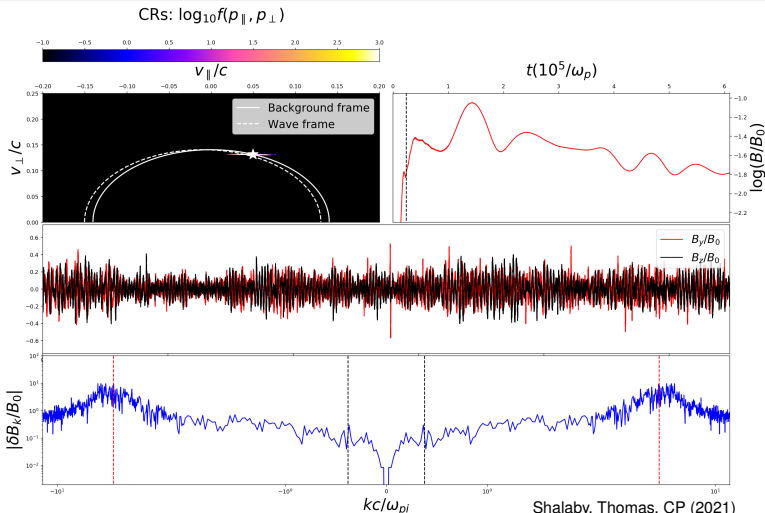
Shalaby, Thomas, CP (2021)

- for  $v_{dr} > \sqrt{\frac{m_i}{m_e}} \frac{v_A}{2}$ : intermediate-scale instability quenched



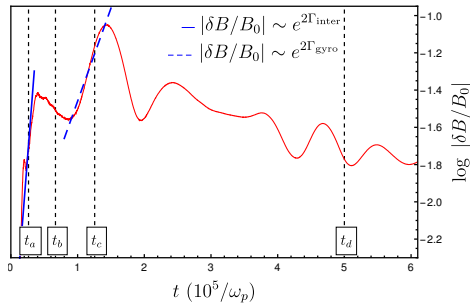
# Cosmic ray driven instabilities

Growth of the intermediate-scale and the gyro-resonant instability



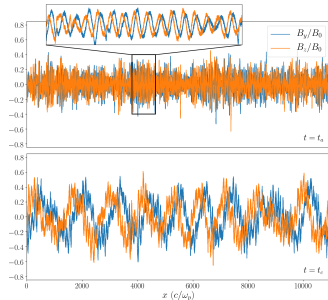
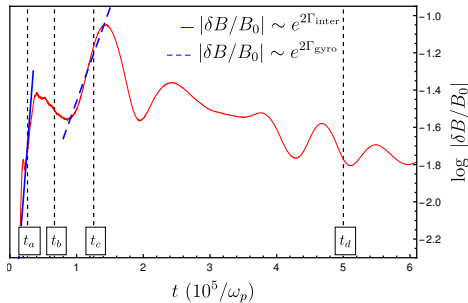
Shalaby, Thomas, CP (2021)

# CR driven instabilities: magnetic field growth



Shalaby, Thomas, CP (2021)

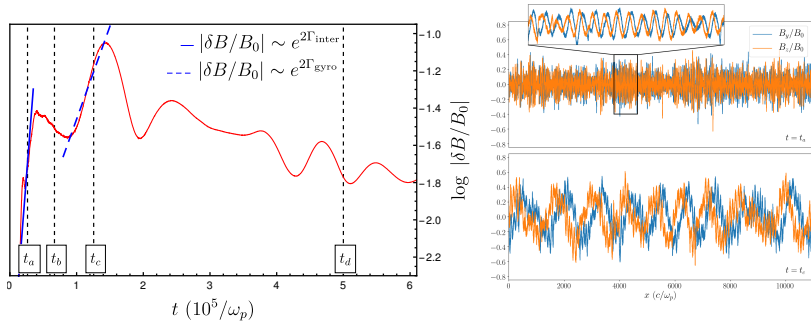
# CR driven instabilities: magnetic field growth



Shalaby, Thomas, CP (2021)

- $t \sim t_a$ : fast magnetic field amplification at scales  $< d_i$

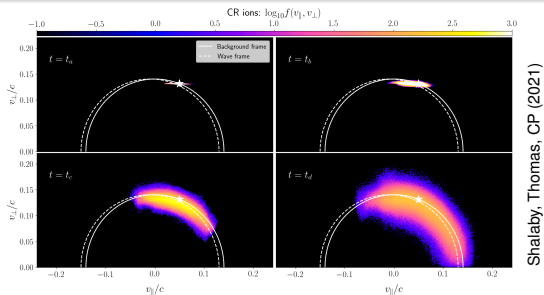
# CR driven instabilities: magnetic field growth



Shalaby, Thomas, CP (2021)

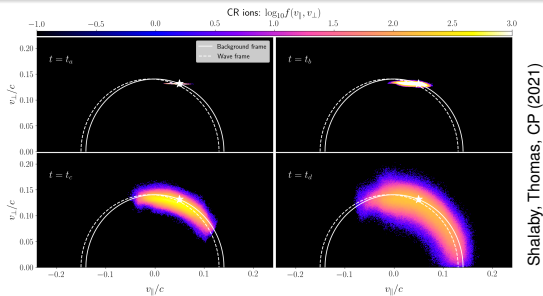
- $t \sim t_a$ : fast magnetic field amplification at scales  $< d_i$
- $t \sim t_c$ : instability starts to grow on larger, gyro-resonant scale  $d_i$

# CR driven instabilities: momentum distribution



Shalaby, Thomas, CP (2021)

# CR driven instabilities: momentum distribution

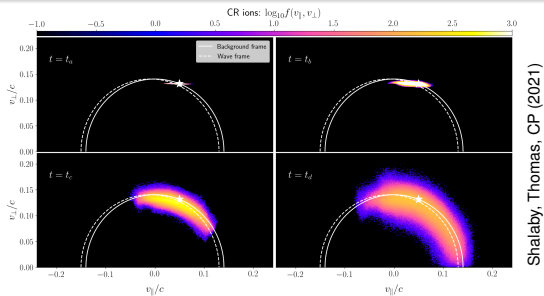


electromagnetic wave with  $v_{ph}$  interacting with particle of velocity  $(v_x, v_y, v_z)$ :

$$\dot{K}_{\parallel} = \frac{m}{2} \frac{dv_x^2}{dt} = qv_x(v_y B_z - v_z B_y)$$

$$\dot{K}_{\perp} = \frac{m}{2} \frac{dv_{\perp}^2}{dt} = -q [(v_x - v_{ph})v_y B_z - (v_x - v_{ph})v_z B_y]$$

# CR driven instabilities: momentum distribution



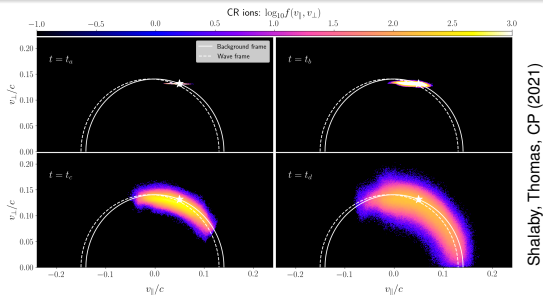
electromagnetic wave with  $v_{ph}$  interacting with particle of velocity  $(v_x, v_y, v_z)$ :

$$\dot{K}_{\parallel} = \frac{m}{2} \frac{dv_x^2}{dt} = qv_x(v_y B_z - v_z B_y)$$

$$\dot{K}_{\perp} = \frac{m}{2} \frac{dv_{\perp}^2}{dt} = -q[(v_x - v_{ph})v_y B_z - (v_x - v_{ph})v_z B_y]$$

•  $t \sim t_a$ :  $v_x \approx v_{ph} \Rightarrow \dot{K}_{\perp} \approx 0$ : parallel scattering only

# CR driven instabilities: momentum distribution



Shalaby, Thomas, CP (2021)

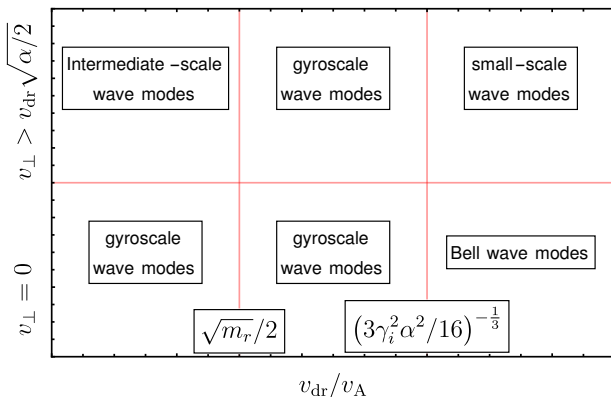
electromagnetic wave with  $v_{ph}$  interacting with particle of velocity  $(v_x, v_y, v_z)$ :

$$\dot{K}_{\parallel} = \frac{m}{2} \frac{dv_x^2}{dt} = qv_x(v_y B_z - v_z B_y)$$

$$\dot{K}_{\perp} = \frac{m}{2} \frac{dv_{\perp}^2}{dt} = -q[(v_x - v_{ph})v_y B_z - (v_x - v_{ph})v_z B_y]$$

- $t \sim t_a$ :  $v_x \approx v_{ph} \Rightarrow \dot{K}_{\perp} \approx 0$ : parallel scattering only
- $t \sim t_c$ :  $v_{ph} \approx 0 \Rightarrow \dot{K}_{\perp} \approx -\dot{K}_{\parallel}$ : energy-conserving scattering

# Regimes of CR driven instabilities



Shalaby, Thomas, CP (2021)

- where  $\alpha = \frac{n_{\text{cr}}}{n_i}$  is the CR number fraction,  $m_r = \frac{m_i}{m_e}$  is the mass ratio, and  $\gamma_i$  is the Lorentz factor of CR ions



AIP

# The intermediate-scale instability

## Properties of the intermediate-scale instability:

- growth rate  $\Gamma_{\text{inter}} \gg \Gamma_{\text{gyro}}$  and excites broad spectral support
- unstable modes are background ion-cyclotron waves in the comoving CR frame

- condition for growth: 
$$\frac{v_{\text{dr}}}{v_A} < \frac{1}{2} \sqrt{\frac{m_i}{m_e}}$$

# The intermediate-scale instability

## Properties of the intermediate-scale instability:

- **growth rate**  $\Gamma_{\text{inter}} \gg \Gamma_{\text{gyro}}$  and excites broad spectral support
- unstable modes are **background ion-cyclotron waves** in the comoving CR frame

- **condition for growth:** 
$$\frac{v_{\text{dr}}}{v_A} < \frac{1}{2} \sqrt{\frac{m_i}{m_e}}$$

## Possible implications of this new instability:

- **enables electron heating at shocks and injection** into diffusive shock acceleration
- couples CRs more tightly to background plasma and **strengthens CR feedback** in galaxies and galaxy clusters
- **slows down CR escape** from the sites of particle acceleration  
→ **brighter gamma-ray halos**



# Electron acceleration at non-relativistic shocks

## ***electron injection problem:***

- gyro-radii:  $r_e = \frac{m_e}{m_i} r_i \Rightarrow$  electrons do *random walk* through the shock transition; no coherent electrostatic shock potential



# Electron acceleration at non-relativistic shocks

## ***electron injection problem:***

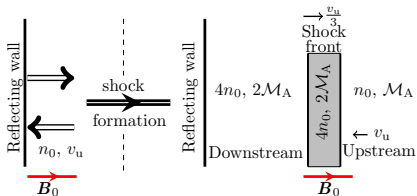
- gyro-radii:  $r_e = \frac{m_e}{m_i} r_i \Rightarrow$  electrons do *random walk* through the shock transition; no coherent electrostatic shock potential
- intermediate-scale instability provides large-amplitude magnetic fluctuations at sub ion-gyroscale



# Electron acceleration at non-relativistic shocks

## *electron injection problem:*

- gyro-radii:  $r_e = \frac{m_e}{m_i} r_i \Rightarrow$  electrons do *random walk* through the shock transition; no coherent electrostatic shock potential
- intermediate-scale instability provides large-amplitude magnetic fluctuations at sub ion-gyroscale  $\Rightarrow$  **a solution? PIC simulations**

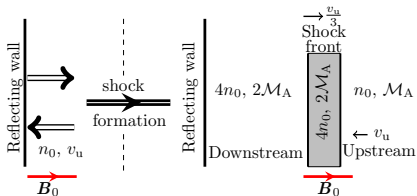


Shalaby, Lemmerz, Thomas, CP (2022):  
 quasi-parallel, non-relativistic shock with PIC code SHARP

# Electron acceleration at non-relativistic shocks

## electron injection problem:

- gyro-radii:  $r_e = \frac{m_e}{m_i} r_i \Rightarrow$  electrons do *random walk* through the shock transition; no coherent electrostatic shock potential
- intermediate-scale instability provides large-amplitude magnetic fluctuations at sub ion-gyroscale  $\Rightarrow$  **a solution? PIC simulations**



Shalaby, Lemmerz, Thomas, CP (2022):  
 quasi-parallel, non-relativistic shock with PIC code SHARP

**Table 1**  
 Parameters of our electron-ion parallel shock simulations

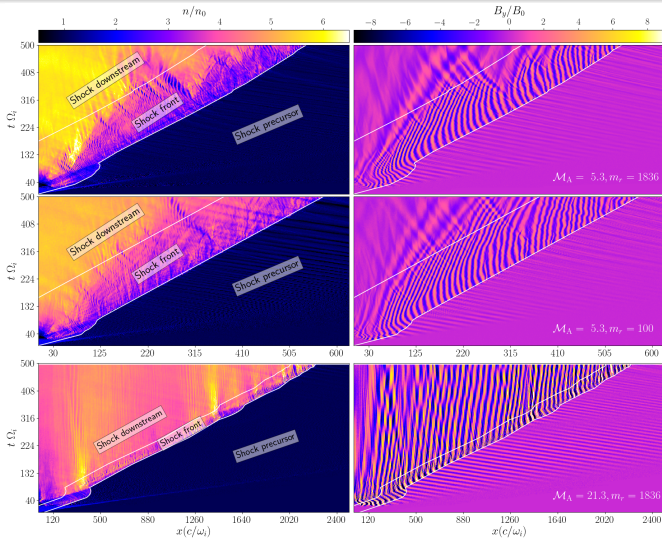
| Name       | $v_u/c^a$ | $\mathcal{M}_A^b$ | $\mathcal{M}_s^c$ | $m_i/m_e$ | Condition <sup>d</sup> |
|------------|-----------|-------------------|-------------------|-----------|------------------------|
| Ma5Mr1836  | -0.1      | 5.3               | 365               | 1836      | ✓                      |
| Ma5Mr100   | -0.1      | 5.3               | 365               | 100       | ×                      |
| Ma21Mr1836 | -0.1      | 21.3              | 365               | 1836      | ×                      |

condition in front/downstream:

$$\mathcal{M}_A \lesssim \frac{1}{4} \sqrt{\frac{m_i}{m_e}}$$



# Shock physics: magnetic amplification

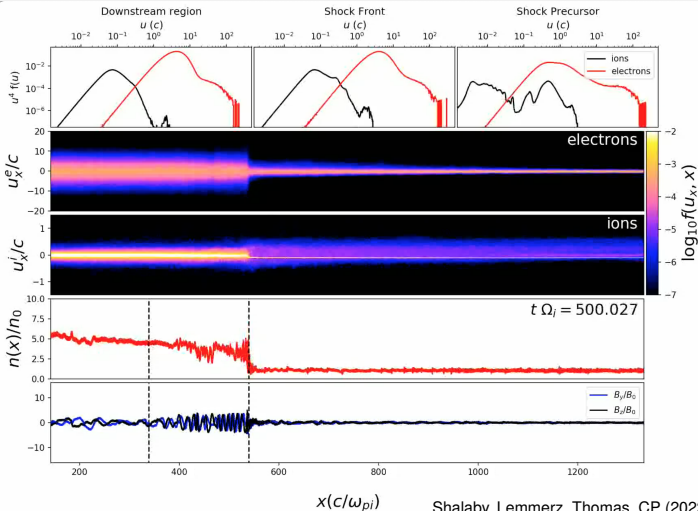


Shalaby, Lemmerz, Thomas, CP (2022)



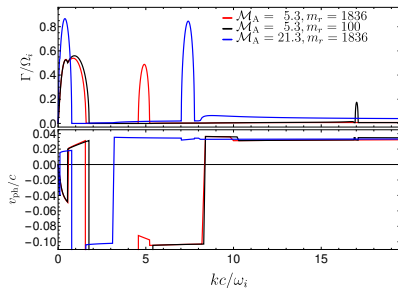
# Particle acceleration at a non-relativistic shock

The intermediate-scale and the gyro-resonant instabilities mediate particle scattering



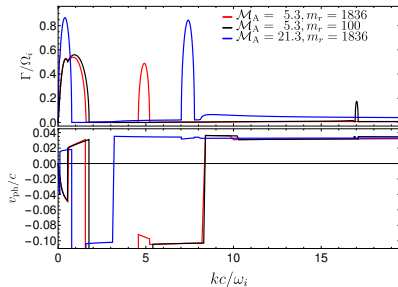
Shalaby, Lemmerz, Thomas, CP (2022)

# Shock acceleration: intermediate-scale instability

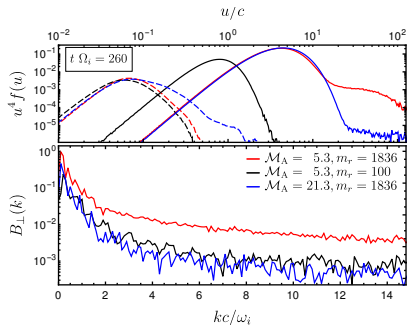


- solution of dispersion relation at shock front (in the contact discontinuity rest frame)

# Shock acceleration: intermediate-scale instability



- solution of dispersion relation at shock front (in the contact discontinuity rest frame)

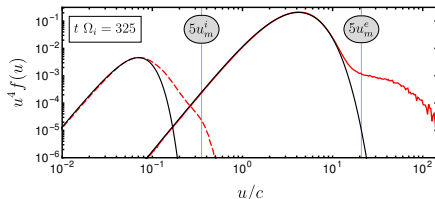


Shalaby, Lemmerz, Thomas, CP (2022)

- only **red** simulation, which grows intermediate-scale instability, accelerates electrons and amplifies magnetic field

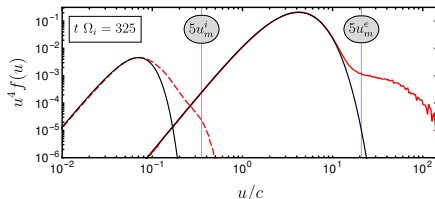


# Shock acceleration efficiency: $K_{ei}$



- rest-frame momentum distribution of ions and electrons
- analytical Maxwell-Jüttner distribution normalized to  $u_m$ , for which  $u^4 f(u)$  is maximum

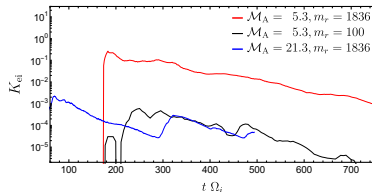
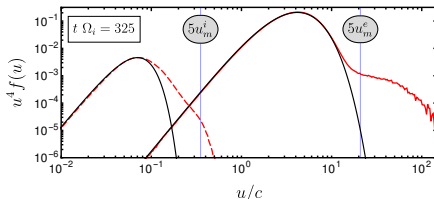
# Shock acceleration efficiency: $K_{ei}$



- rest-frame momentum distribution of ions and electrons
- analytical Maxwell-Jüttner distribution normalized to  $u_m$ , for which  $u^4 f(u)$  is maximum
- non-thermal electron-to-ion energy:

$$K_{ei} = \frac{E_e(u > 5u_m^e)}{E_i(u > 5u_m^i)}$$

# Shock acceleration efficiency: $K_{ei}$



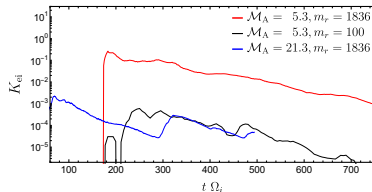
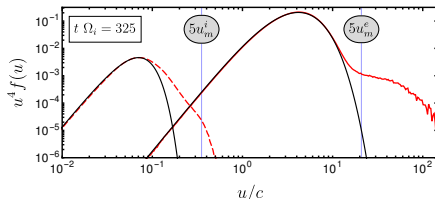
Shalaby, Lemmerz, Thomas, CP (2022)

- rest-frame momentum distribution of ions and electrons
- analytical Maxwell-Jüttner distribution normalized to  $u_m$ , for which  $u^4 f(u)$  is maximum
- non-thermal electron-to-ion energy:

$$K_{ei} = \frac{E_e(u > 5u_m^e)}{E_i(u > 5u_m^i)}$$

- downstream evolution of  $K_{ei}$  (non-thermal ion distribution still growing)
- $\mathcal{M}_s$  and  $v_{sh}$  identical for all runs, only  $\mathcal{M}_A$  differs

# Shock acceleration efficiency: $K_{ei}$



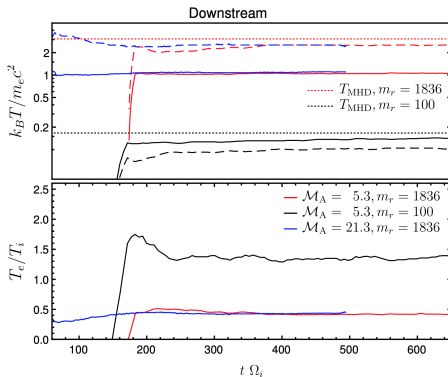
Shalaby, Lemmerz, Thomas, CP (2022)

- rest-frame momentum distribution of ions and electrons
- analytical Maxwell-Jüttner distribution normalized to  $u_m$ , for which  $u^4 f(u)$  is maximum
- non-thermal electron-to-ion energy:

$$K_{ei} = \frac{E_e(u > 5u_m^e)}{E_i(u > 5u_m^i)}$$

- downstream evolution of  $K_{ei}$  (non-thermal ion distribution still growing)
- $\mathcal{M}_s$  and  $v_{sh}$  identical for all runs, only  $\mathcal{M}_A$  differs
- presence of intermediate-scale instability increases  $K_{ei}$  by more than 100!**

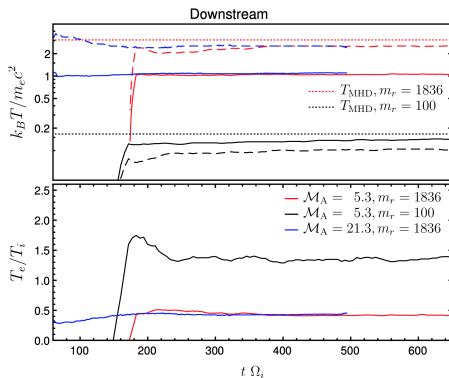
# Shock dissipation: electron and ion temperatures



Shalaby, Lemmerz, Thomas, CP (2022)

- time evolution of downstream  $T_i$  (dashed) and  $T_e$  (solid)

# Shock dissipation: electron and ion temperatures

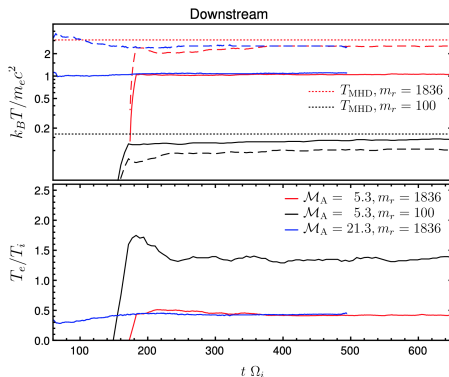


Shalaby, Lemmerz, Thomas, CP (2022)

- time evolution of downstream  $T_i$  (dashed) and  $T_e$  (solid)

- runs with  $m_i/m_e = 1836$  have different efficiencies  $K_{ei}$  but same temperatures

# Shock dissipation: electron and ion temperatures

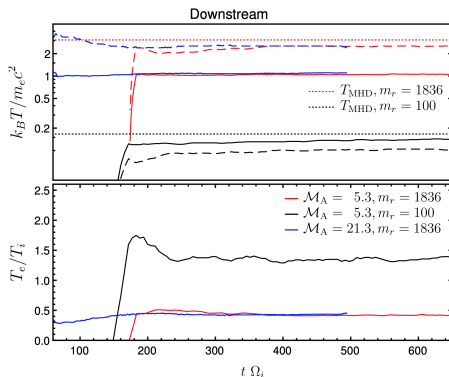


Shalaby, Lemmerz, Thomas, CP (2022)

- time evolution of downstream  $T_i$  (dashed) and  $T_e$  (solid)

- runs with  $m_i/m_e = 1836$  have different efficiencies  $K_{ei}$  but same temperatures
- $T_i$  equilibrates to MHD value (deviations due to CR and magnetic energies)
- $T_e \approx 0.4 T_i$  (1D vs. 3D or missing instabilities?)

# Shock dissipation: electron and ion temperatures



Shalaby, Lemmerz, Thomas, CP (2022)

- time evolution of downstream  $T_i$  (dashed) and  $T_e$  (solid)

- runs with  $m_i/m_e = 1836$  have different efficiencies  $K_{ei}$  but same temperatures
- $T_i$  equilibrates to MHD value (deviations due to CR and magnetic energies)
- $T_e \approx 0.4 T_i$  (1D vs. 3D or missing instabilities?)
- true  $m_i/m_e$  required for correct heating physics

# Electron acceleration at non-relativistic shocks

## Intermediate-scale instability at shocks:

- provides efficient pre-acceleration that scatters and accelerates electrons on scales much shorter than the ion gyro radius
- instability drives comoving ion-cyclotron waves (with the upstream plasma) at the shock front

- condition for growth:  $\frac{v_{\text{sh}}}{v_{A,0}} < \frac{1}{4} \sqrt{\frac{m_i}{m_e}}$ , for  $n = 4n_0$



# Electron acceleration at non-relativistic shocks

## Intermediate-scale instability at shocks:

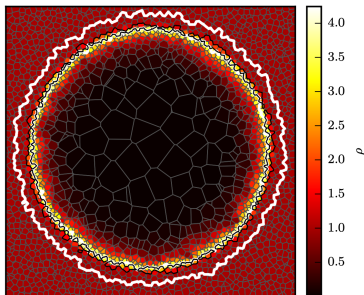
- provides efficient pre-acceleration that scatters and accelerates electrons on scales much shorter than the ion gyro radius
- instability drives comoving ion-cyclotron waves (with the upstream plasma) at the shock front
- condition for growth:  $\frac{v_{\text{sh}}}{v_{A,0}} < \frac{1}{4} \sqrt{\frac{m_i}{m_e}}$ , for  $n = 4n_0$

## Electron shock acceleration and heating:

- intermediate-scale instability increases electron acceleration efficiency (by factor  $> 100$ )
- ion thermalization in line with MHD (accounting for  $E_B$  and  $E_{\text{CR}}$ ), but  $T_e \approx 0.4 T_i$  remains open question
- reduced  $m_i/m_e$  suppresses intermediate instability, precludes electron acceleration, results in erroneous electron and ion heating



# Global MHD simulations of SNRs with CR physics

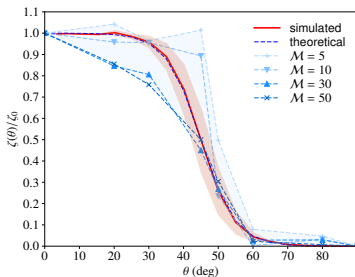


- detect and characterize shocks and jump conditions on the fly

Mach number finder with CRs

CP+ (2017)

# Global MHD simulations of SNRs with CR physics



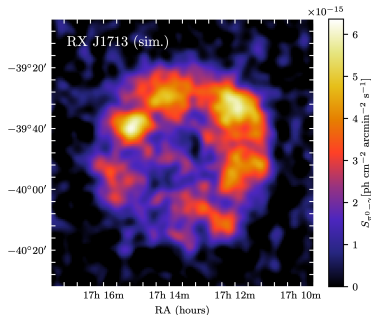
- detect and characterize shocks and jump conditions on the fly
- measure Mach number  $\mathcal{M}$  and magnetic obliquity  $\theta_B$

obliquity-dep. acceleration efficiency

Pais, CP+ (2018) based on

hybrid PIC sim.'s by Caprioli & Spitkovsky (2015)

# Global MHD simulations of SNRs with CR physics

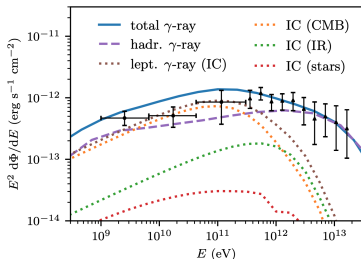


- detect and characterize shocks and jump conditions on the fly
- measure Mach number  $\mathcal{M}$  and magnetic obliquity  $\theta_B$
- inject and transport CR protons  
⇒ dynamical back reaction on gas flow, hadronic emission

simulated TeV gamma-ray map

Pais & CP (2020)

# Global MHD simulations of SNRs with CR physics

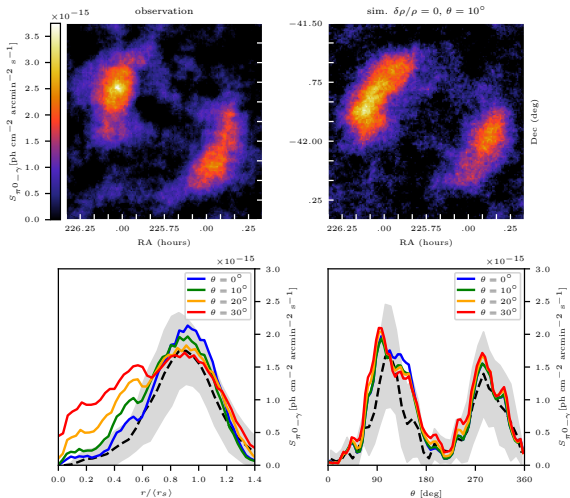


simulated gamma-ray spectrum

Winner, CP+ (2019, 2020)

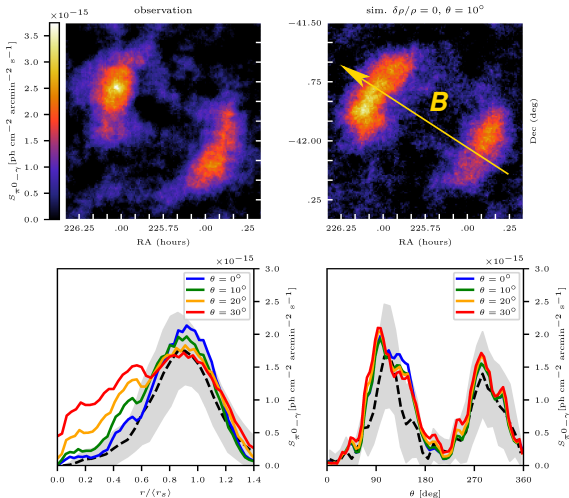
- detect and characterize shocks and jump conditions on the fly
- measure Mach number  $\mathcal{M}$  and magnetic obliquity  $\theta_B$
- inject and transport CR protons  
⇒ dynamical back reaction on gas flow, hadronic emission
- inject and transport CR electrons
- calculate non-thermal radio, X-ray,  $\gamma$ -ray emission

# Hadronic TeV $\gamma$ rays: SN 1006



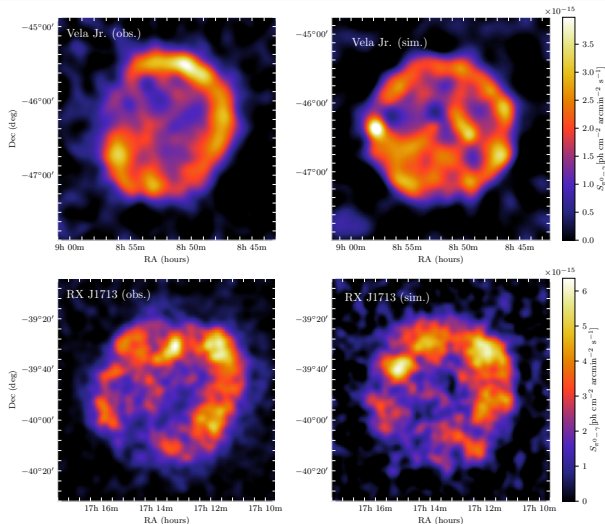
Pais & CP (2020)

# Hadronic TeV $\gamma$ rays: SN 1006



Pais & CP (2020)

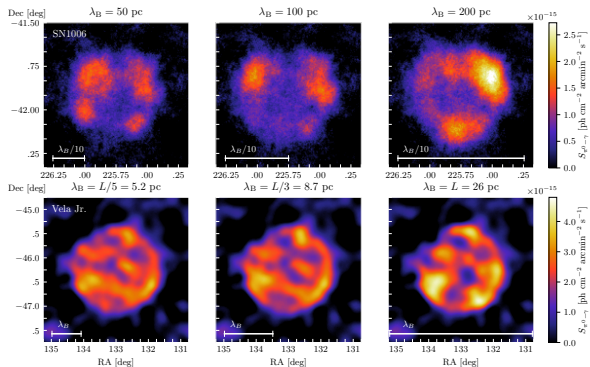
# Hadronic TeV $\gamma$ rays: Vela Jr. and RXJ 1713



Pais & CP (2020)

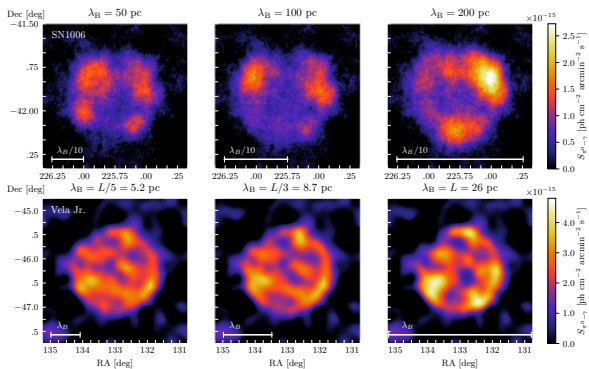
# TeV $\gamma$ rays from shell-type supernova remnants

Varying magnetic coherence scale in simulations of SN 1006 and Vela Junior



# TeV $\gamma$ rays from shell-type supernova remnants

Varying magnetic coherence scale in simulations of SN 1006 and Vela Junior



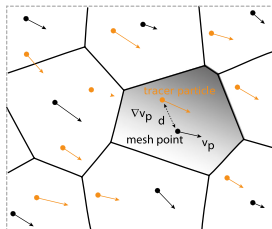
Pais, CP+ (2020)

$\Rightarrow$  Correlation structure of **patchy TeV  $\gamma$ -rays constrains magnetic coherence scale in ISM:**

SN 1006:  $\lambda_B > 200_{-10}^{+80}$  pc

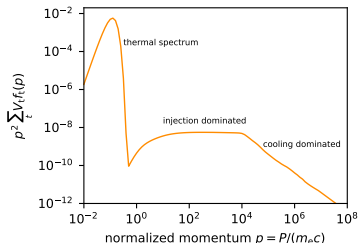
Vela Junior:  $\lambda_B = 13_{-4.3}^{+13}$  pc

# CREST - Cosmic Ray Electron Spectra evolved in Time



**CREST code** (Winner, CP+ 2019)

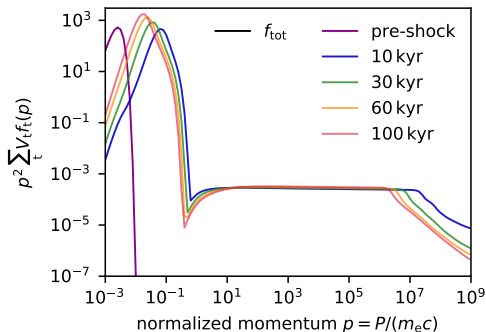
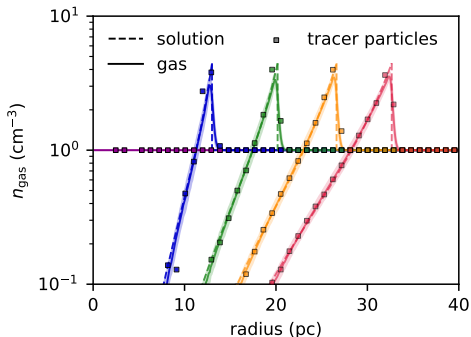
- post-processing MHD simulations
- on Lagrangian particles
  - adiabatic processes
  - Coulomb and radiative losses
  - Fermi-I (re-)acceleration
  - Fermi-II reacceleration
  - secondary electrons



**Link to observations**

- radio synchrotron
- inverse Compton (IC)  $\gamma$ -ray

# Sedov–Taylor blast wave: spectral evolution

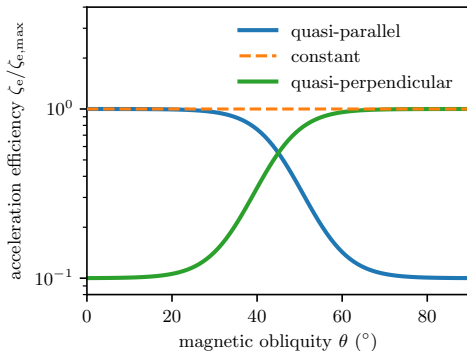


$$E_0 = 10^{51} \text{ erg}, n_{\text{gas}} = 1 \text{ cm}^{-3}, T_0 = 10^4 \text{ K}, B = 1 \mu\text{G}$$

Winner, CP+ (2019)



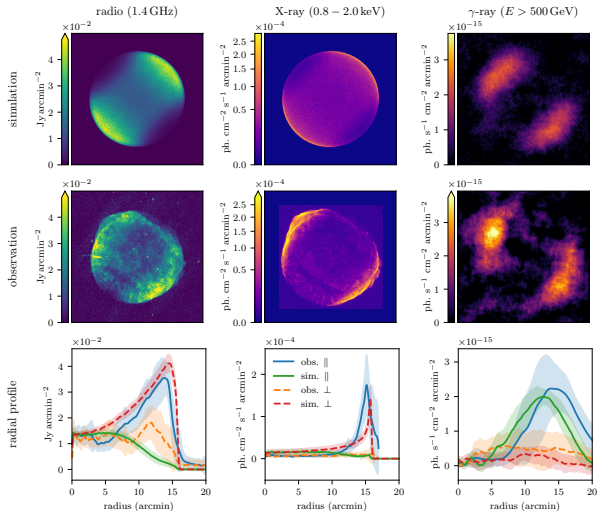
# SN 1006: CR electron acceleration models



Winner, CP+ (2020)

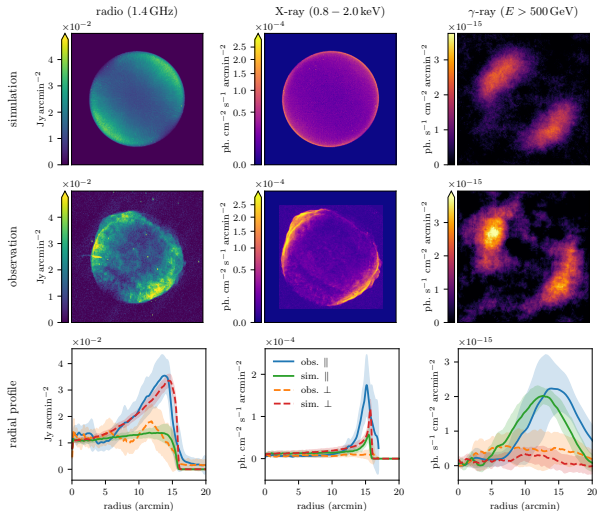
- different obliquity dependent electron acceleration efficiencies:
  1. preferred quasi-perpendicular acceleration (previous PIC)
  2. constant acceleration efficiency (a straw man's model)
  3. preferred quasi-parallel acceleration (like CR protons)

# CR electron acceleration: quasi-perpendicular shocks



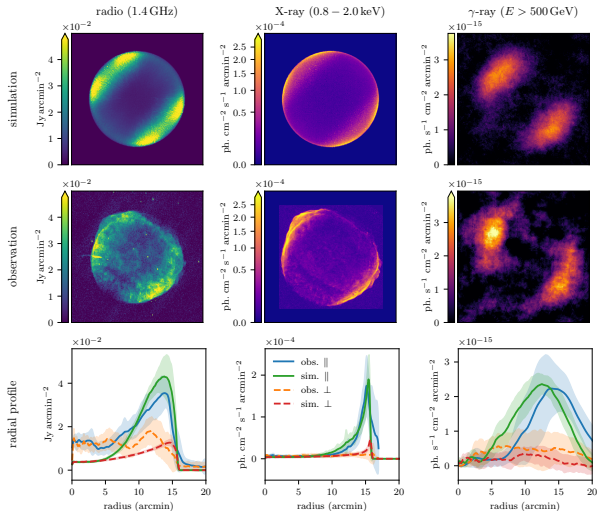
Winner, CP+ (2020)

# CR electron acceleration: constant efficiency



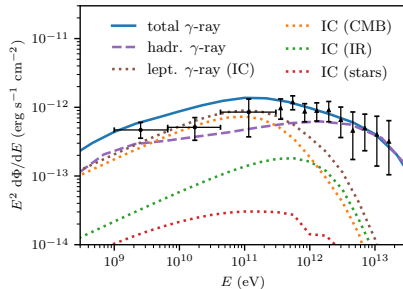
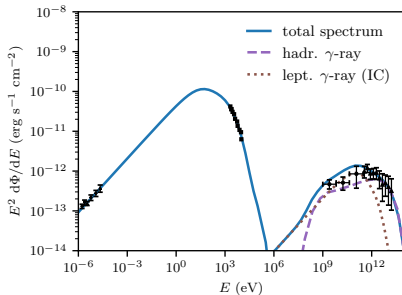
Winner, CP+ (2020)

# CR electron acceleration: quasi-parallel shocks



Winner, CP+ (2020)

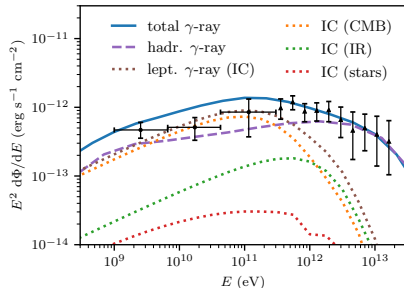
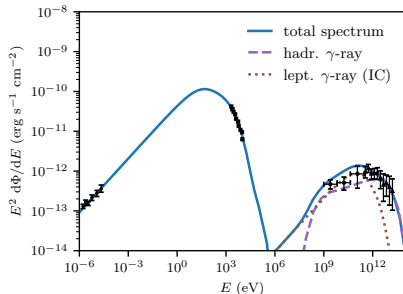
# SN 1006: multi-frequency spectrum



Winner, CP+ (2020)

- quasi-parallel acceleration model fits multi-frequency spectrum

# SN 1006: multi-frequency spectrum



Winner, CP+ (2020)

- quasi-parallel acceleration model fits multi-frequency spectrum
- GeV regime: leptonic inverse Compton dominates
- TeV regime: hadronic pion decay

# Conclusions for CR hydrodynamics at SNRs

## CR hydrodynamics with kinetic plasma physics:

- Shock finder enables CR acceleration in MHD simulations
- CR proton transport in MHD enables dynamic backreaction
- CR electron spectral transport (CREST): multi-frequency spectra and emission maps

# Conclusions for CR hydrodynamics at SNRs

## CR hydrodynamics with kinetic plasma physics:

- Shock finder enables CR acceleration in MHD simulations
- CR proton transport in MHD enables dynamic backreaction
- CR electron spectral transport (CREST): multi-frequency spectra and emission maps

## CR acceleration constraints by MHD models:

- TeV shell-type SNRs probe magnetic coherence scale in ISM
- hybrid-PIC simulations of  $p^+$  acceleration agree with global SNR simulations
- global SNR simulations imply preferred quasi-parallel  $e^-$  acceleration: new intermediate instability enables  $e^-$  (pre-)acceleration



Cosmic ray driven instabilities  
Electron acceleration at shocks  
Supernova remnant simulations

MHD setup  
Protons and hadronic emission  
Electrons and leptonic emission

# PICO GAL: From Plasma Kinetics to COsmological GALaxy Formation



This project has received funding from the European Research Council (ERC) under the European Union's Horizon 2020 research and innovation program (grant agreement No PICO GAL-101019746).

Christoph Pfrommer

Particle acceleration at non-relativistic shocks



# Literature for the talk – 1

## Cosmic ray driven instabilities:

- Shalaby, Thomas, Pfrommer, *A new cosmic ray-driven instability*, 2021, ApJ, 908, 206.
- Shalaby, Lemmerz, Thomas, Pfrommer, *The mechanism of efficient electron acceleration at parallel non-relativistic shocks*, 2022, ApJ, 932, 86.

## Cosmic ray hydrodynamics and shock acceleration:

- Pfrommer, Pakmor, Schaal, Simpson, Springel, *Simulating cosmic ray physics on a moving mesh* 2017, MNRAS, 465, 4500.



# Literature for the talk – 2

## Cosmic ray electron spectra in MHD:

- Winner, Pfrommer, Girichidis, Pakmor, *Evolution of cosmic ray electron spectra in magnetohydrodynamical simulations*, 2019, MNRAS, 488, 2235.
- Winner, Pfrommer, Girichidis, Werhahn, Pais, *Evolution and observational signatures of the cosmic ray electron spectrum in SN 1006*, 2020, MNRAS, 499, 2785.

## Cosmic ray proton acceleration at SNRs:

- Pais, Pfrommer, Ehlert, Pakmor, *The effect of cosmic-ray acceleration on supernova blast wave dynamics*, 2018, MNRAS, 478, 5278.
- Pais, Pfrommer, Ehlert, Werhahn, Winner, *Constraining the coherence scale of the interstellar magnetic field using TeV gamma-ray observations of supernova remnants*, 2020, MNRAS, 496, 2448.
- Pais, Pfrommer, *Simulating TeV gamma-ray morphologies of shell-type supernova remnants*, 2020, MNRAS, 498, 5557.